Microchimica Acta (2021) 188: 129
https://doi.org/10.1007/s00604-021-04783-4

ORIGINAL PAPER

Rapid and simple colorimetric detection of hydrogen sulfide using an etching-resistant effect on silver nanoprisms

Yong Jin Ahn[1] · Seong Hyun Han[1] · Gi-Ja Lee[1,2]

Received: 3 December 2020 / Accepted: 10 March 2021 / Published online: 19 March 2021

Abstract

A fast and sensitive colorimetric paper sensor has been developed using silver nanoprisms (Ag NPRs) with an edge length of ~50 nm for the detection of free H_2S gas. We prepared two types of Ag NPRs-coated H_2S sensing papers: a multi-zone patterned paper for passive (diffusion mode), and a single-zone patterned paper for pumped mode of H_2S gas. The change in color intensity was quantitatively analyzed of Ag NPRs-coated paper after KCl treatment depending on the concentration of H_2S gas, from yellow to purplish brown. As a result, Ag NPRs-coated H_2S sensing paper showed good sensitivity with a linear range of 1.03 to 32.9 μM H_2S, high selectivity, and good reproducibility and stability, together with a fast response time of 1 min. The developed H_2S sensing paper was applied to detect the free H_2S gas released from three types of garlic including crushed, peeled, and fresh garlic. Therefore, it can be utilized as a simple, fast, and reliable tool for on-site colorimetric detection of free H_2S gas for quality control of dietary supplements and exhaled breath analysis.

Keywords Hydrogen sulfide gas · Silver nanoprisms · Etching-resistance · Sensing paper · Colorimetric detection

Introduction

Hydrogen sulfide (H_2S) is a colorless gas with a characteristic odor of rotten eggs, and high levels of H_2S are corrosive and toxic [1, 2]. However, low concentrations of H_2S act as a gaseous signaling molecule in the human body, like carbon monoxide or nitric oxide. Abnormal levels of H_2S in the human body cause breathing problems, such as shortness of breath and respiratory paralysis [3]. In addition, defects in H_2S levels in the human body cause problems with pathophysiological functions, such as vasodilation [4] and neuromodulation [5], and lead to developmental disorder, diabetes [6], and Alzheimer's disease [7]. H_2S is also present in foods such as dairy products, wine, and meat, which greatly affects the state of the product in relation to taste and aroma [8]. In addition, H_2S in exhaled breath is considered a potential biomarker for non-invasive and rapid assessment of small intestinal bacterial overgrowth in irritable bowel syndrome patients [9]. As volatile sulfur compounds, such as H_2S and methyl mercaptan, are mainly responsible for intraoral halitosis [10], sulfur monitoring in the breath has most commonly been used for the diagnosis of halitosis. Therefore, it is necessary to develop sensitive and selective methods for H_2S gas detection in foods and biological samples, such as serum and exhaled breath.

Various analytical methods, such as electrochemical analysis [11, 12], metal-induced sulfide precipitation [13], gas chromatography [14], and liquid chromatography analysis [15], have been used to detect H_2S. However, these methods mostly require expensive instruments, complicated sample pretreatments, and long analysis time. Colorimetric detection has been regarded as one of the most convenient and powerful techniques for the on-site analysis of H_2S, in terms of miniaturization, simplicity, and cost efficiency. In addition, when in the visible range, the analyte can be quickly detected with the naked eye [16, 17].

Recently, silver nanoprisms (Ag NPRs), also referred to as nanoplates (NPls) or nanodisks (NDs), have attracted increasing interest as chemical and biological sensors, because of their rich optical properties, which originate from their extreme geometric anisotropy [18]. They exhibit three localized

✉ Gi-Ja Lee
gjlee@khu.ac.kr

[1] Department of Medical Engineering, Graduate School, Kyung Hee University, Seoul 02447, Republic of Korea

[2] Department of Biomedical Engineering, College of Medicine, Kyung Hee University, 26, Kyungheedae-ro, Dongdaemun-gu, Seoul 02447, Republic of Korea

surface plasmon resonance (LSPR) peaks in the UV-Vis spectrum, corresponding to out-of-plane quadrupole (330 nm; peak), in-plane quadrupole (400 nm; shoulder), and in-plane dipole (780 nm; peak) modes [19]. Among them, the wavelength of the in-plane dipole LSPR mode of Ag NPRs can be tuned by adjusting the aspect ratios and corner sharpness to cover almost the entire visible spectrum to the near-IR [18, 20]. Although Ag NPRs are etched by heat [21] and UV light irradiation [22], oxidative etching using an etchant, such as halide ions, is one of the most effective ways for the shape control of Ag NPRs [23]. These characteristics of Ag NPRs can be utilized to detect sulfur-containing compounds, because they can cause anti-etching effect on Ag NPRs against an etchant. For example, Li et al. [24] reported a "red-to-blue" colorimetric detection of cysteine via anti-etching of Ag NPR solution. They utilized the cysteine effect that can prevent iodide ions (I^-) attack from attachment to the surface of Ag NPRs. Zhang et al. [23] reported a colorimetric captopril assay based on oxidative etching-directed morphology control of Ag NPRs. This assay used an etching strategy by which captopril can effectively prevent the morphological transition from triangular prism to rounded disk. Although anti-etching strategies have been applied to the detection of sulfur-containing biomolecules in solutions using UV-Vis spectra, to the best of our knowledge, the colorimetric paper sensor using an etching-resistant effect on Ag NPRs for the selective and sensitive detection of free H_2S gas has yet to be reported.

In this study, we introduce a fast and sensitive colorimetric paper sensor using Ag NPRs for the detection of free H_2S gas. The detection principle is that Ag NPRs on the paper react with H_2S gas to form Ag_2S on their surfaces, which induces etching-resistant Ag NPRs against Cl^- ions. As a result, the color of Ag NPRs on the paper after KCl treatment varies from yellow to purplish brown, depending on the concentration of H_2S gas. We prepared two types of Ag NPRs-coated paper sensors for the detection of H_2S gas. One is a multi-zone patterned H_2S sensing paper for passive (diffusion) mode, which can be placed on 96-well microplates, and covered with a microplate cover. The other is a single-zone patterned H_2S sensing paper for pumped mode, which can be inserted within a holder, and connected to a syringe and a pump. In this case, H_2S gas released from the H_2S donor solution or sample within a beaker is collected by syringe. First, we optimized the synthesis conditions for the Ag NPRs and the fabrication conditions for the Ag NPRs-coated H_2S sensing papers, together with the concentration of the added KCl. We evaluated the analytical performance as a colorimetric H_2S sensor, using the parameter b intensity of L*a*b color space. Finally, we successfully measured the H_2S levels released from three types of garlic including crushed, peeled, and fresh garlic according to its weight within 1 min. Scheme 1 illustrates the experimental scheme.

Experimental

Materials and chemicals

Silver nitrate ($AgNO_3$), trisodium citrate, sodium borohydride ($NaBH_4$), sodium polystyrene sulfonate (PSS), hydrogen peroxide (H_2O_2, 30% *w*/w in H_2O), sulfuric acid (H_2SO_4), L-ascorbic acid (AA), sodium sulfide (Na_2S), dithiothreitol (DTT), glutathione (GSH), nitric oxide (NO), cysteine (Cys), 4-aminothiophenol (4-ATP), and homocysteine (H-cys) were purchased from Sigma-Aldrich (St. Louis, MO, USA). All reagents were of analytical grade, and were used without further purification. All aqueous solutions were prepared using distilled water of 18.2 MΩ·cm resistivity from the Millipore Direct-Q water supply system.

Whatman® filter paper (grade 1; 200 mm × 200 mm) was purchased from GE Healthcare Life Sciences (Tokyo, Japan), and a 96-well microplate was obtained from SPL Life Sciences (Pocheon, Gyeonggi-do, Korea). Lead acetate paper was purchased from Precision Laboratories (Cottonwood, AZ, USA).

Fabrication of wax patterned paper substrates

The two types of paper substrates were designed using AutoCAD, as follows: First, the multi-zone patterned paper is 126 mm in width, 81 mm in length, and 0.18 mm in thickness. It contains 24 circular detection areas, each of 7 mm inner diameter (Fig. S1(A) of the Supplementary Information (SI)). The multi-zone patterned paper can be inserted between a microplate and a cover to detect H_2S gas that is released from Na_2S standard solution as the H_2S donor within wells. To reduce the error by gas diffusion, detection zones were spaced 9 mm apart. Next, the single-zone patterned paper is a perfect circle with 21 mm diameter (Fig. S1(B) of the SI). One detection area with a 6 mm inner diameter is in the center. The paper is placed within a holder that can connect with a syringe. Hydrophobic wax barriers were printed using a Xerox ColorCube 8570 N printer (Fuji Xerox, Tokyo, Japan). Uniform impregnation of wax on the Whatman filter paper was performed in a BF-150C drying oven (DAIHAN Scientific, Seoul, Korea)) at 130 °C for 90 s. Finally, the wax patterned paper was removed from the oven, and cooled rapidly to room temperature (RT).

Synthesis of Ag NPRs

Prior to the synthesis, all 50 mL glassware was cleaned with a piranha solution (3:1 (v/v) H_2SO_4/H_2O_2), rinsed thoroughly in distilled water, and dried in oven at 90 °C. Ag NPRs were synthesized through a slight modification of a reproducible seed-based method in the following procedures [26]. Briefly, Ag seeds were produced by mixing aqueous trisodium citrate

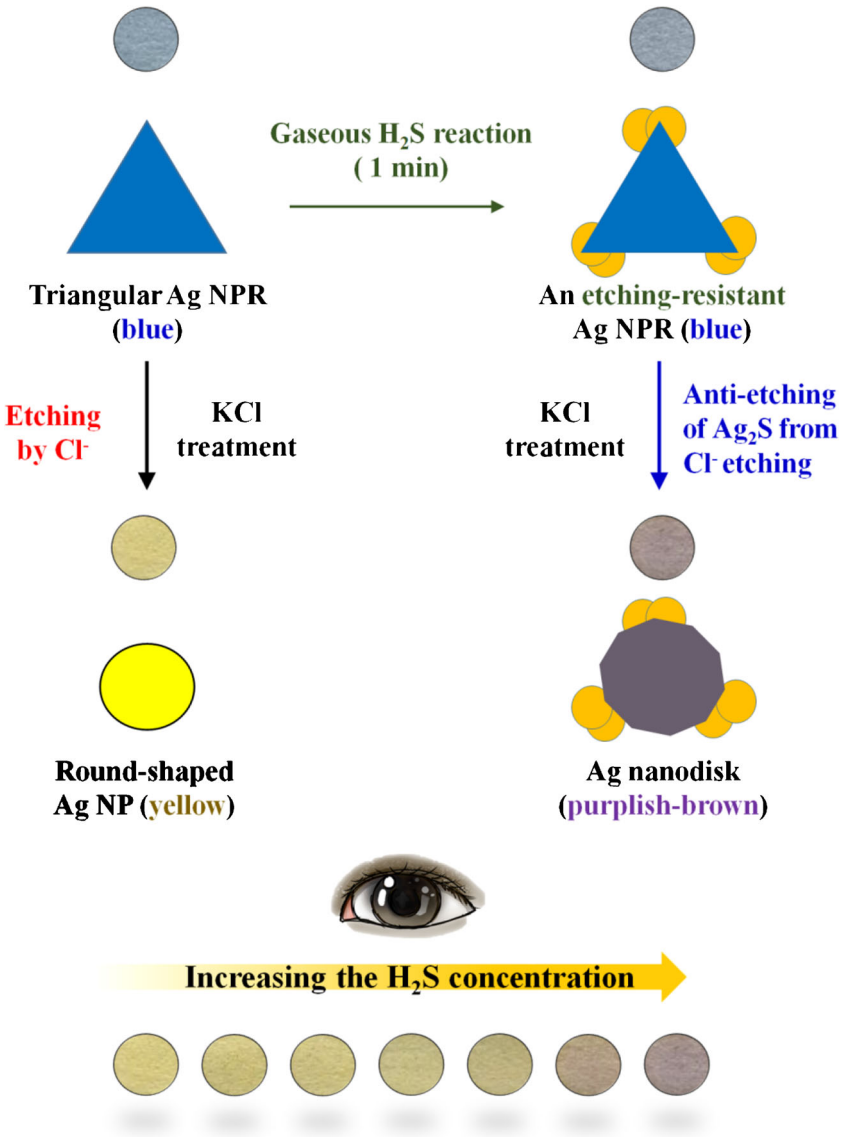

Scheme 1 Schematic of the paper-based colorimetric detection of hydrogen sulfide (H_2S) gas utilizing an etching-resistant effect of H_2S on silver nanoprisms (Ag NPRs)

(5 mL, 1.5 mM), PSS (0.25 mL, 0.1 mM), and $NaBH_4$ (0.3 mL, 10 mM, freshly prepared), followed by the addition of $AgNO_3$ solution (6 mL, 0.5 mM) at a rate of 2 mL/min while continuously stirring for 20 min, to obtain yellow seed solution. The prepared Ag seeds were used without any further purification or concentration for the Ag NPRs growth step.

To synthesize Ag NPRs via the seed growth method, 20 mL of 0.15 mM AA was added to the as-prepared Ag seeds solution (400 μL) under vigorous stirring. Then, 12 mL of 0.5 mM $AgNO_3$ was injected into this mixture at a rate of 1 mL/min. After injection of $AgNO_3$, the color changed from transparent to yellow, and further to red and blue, indicating the formation of the Ag NPRs with an extinction spectrum of 740 nm. The as-prepared Ag NPRs solution was centrifuged at 3700 g for 20 min to remove the residue polymer material and reducing agent. The resultant Ag NPRs were re-dispersed in 3 mM trisodium citrate. The final stock Ag NPRs solution was concentrated to OD 1.0 (diluted 60-fold) for colorimetric and spectroscopic application. The resulting Ag NPRs were stored in the dark at 4 °C before use. All absorbance measurements were performed using a Synergy HTX multi-mode reader (BioTek, Winooski, VT, USA).

Preparation and characterization of Ag NPRs-coated paper

To prepare the H_2S sensing paper, an aliquot of 7 μL of the prepared Ag NPR solution with blue color was carefully dropped onto each detection zone within the two types of wax-patterned papers with the multi-zone and the single zone, respectively. This Ag NPR-coated paper was dried in a constant temperature and humidity chamber ((23.5 ± 1.0) °C, (25.0 ± 5.0) %) for 10 min. To optimize the fabrication

conditions of sensing paper for the colorimetric detection of H_2S gas, we varied the maximum localized surface plasmon resonance wavelength ($LSPR_{\lambda max}$) as 560, 600, 750, 820, and 960 nm and the loading volume as 3, 4, 5, 6, 7, and 8 μL of Ag NPRs solutions. We changed the reaction time between Ag NPRs and H_2S gas as 1, 2.5, 5, 7, and 10 min, and the concentration of KCl as 0.01, 0.1, 1, 10, 100, and 1000 mM.

The optimized H_2S sensing paper coated with Ag NPRs was characterized by field emission scanning electron microscopy (FE-SEM; LEO SUPRA 55, Carl Zeiss, Oberkochen, Germany), and SERSRA confocal Raman spectroscopy (Bruker Optics, Billerica, MA, USA) with an excitation laser of 785 nm (10 mW power) and ×20 objective lens. The SERS analysis was performed by adding 7 μL of 4-ATP (100 mM) on Ag NPR-coated paper before and after the addition of KCl. After drying at RT for 10 min, the SERS measurements were performed with a spectral resolution of 5 cm^{-1}, and a focal spot size of less than 1 μm. The SERS signal was collected within the fingerprint range of (417–1782) cm^{-1} and the acquisition time of 10 s. The acquisition process was repeated five times in different regions. The obtained data were subtracted from the equipment background, and averaged at five arbitrary points.

Analytical performance of the H_2S sensing paper

The analytical performance of the multi-zone pattered H_2S sensing paper was evaluated by the previously reported procedure, as follows [26, 27]; briefly, a 300 μL of Na_2S solution of 3.1, 6.3, 12.5, 25, 50, and 100 μM in 100 mM phosphate buffered saline (PBS, pH 7.4) was added into each well of the 96-well microplate (Fig. S1(C) of the SI). The Ag NPR-coated H_2S paper was placed on 96-well microplates, and covered with a microplate cover for 1 min at RT. After exposure to H_2S for 1 min, the Ag NPR-coated paper was removed from the 96-well plate. Then, 7 μL of 1 M KCl was dropped onto the detection zone. After 10 min, the changes in color intensity of the Ag NPR-coated paper could be checked with the naked eye, and could also be analyzed quantitatively using an Epson scanner (Perfection V700 Photo flatbed scanner, Seiko Epson, Nagano, Japan) and ImageJ software. The circular core areas on ImageJ measuring 4.5 mm in diameter in each wax-patterned zone were analyzed using the parameter b of the L*a*b color space [27].

To evaluate the analytical performance of the single-zone patterned, Ag NPR-coated H_2S sensing paper, we first inserted it within the easy-pressure syringe filter holder (21 mm diameter), in which inlet and outlet seal plugs were included, together with a rubber O-ring and membrane support screen. After the addition of 10 mL of Na_2S solution into a 500-mL round bottom flask, the flask was capped, and the aqueous solution was vaporized in the flask for 20 min. A 6 mL of vaporized H_2S gas was taken with a disposable plastic syringe/needle (KOVAX Corp., Japan), and the syringe connected to the holder. Subsequently, the H_2S gas within the syringe was injected into the Ag NPRs-coated paper, using a syringe pump (PHD 22/2000 Syringe Pump, Harvard Apparatus, USA) at a constant rate of 6 mL/min (Fig. S1(D) of the SI). After the reaction with H_2S gas, the Ag NPRs-coated paper was taken out of the holder, and 7 μL of 1 M KCl was dropped onto the single detection zone. After 10 min, the changes in color intensity of the single-zone pattered, Ag NPR-coated paper could also be confirmed with the naked eye, and could be analyzed by the same methods as used for the multi-zone patterned paper.

Feasibility test

To evaluate the feasibility of our single-patterned, Ag NPR-coated H_2S sensing paper as a fast and sensitive sensor for the guideline of dietary supplements, it was applied to monitor H_2S gas produced from three kinds of garlic including crushed, peeled, and fresh garlic. The various mass of 50, 100, 150, and 200 g of crushed and peeled garlic, and 100 and 200 g of fresh garlic was inserted into each 500 mL round beaker, and immediately sealed with a rubber cap. After 20 min, 6 mL of the gas was taken with syringe, followed by connection with the holder. Subsequently, the gas within the syringe was injected into the Ag NPR-coated paper within the holder for 1 min, using a syringe pump. After the reaction with the gas for 1 min and the subsequent addition of KCl, the changes in color intensity of the Ag NPR-coated H_2S sensing paper were analyzed quantitatively.

Results and discussion

Characterization of Ag NPRs before and after KCl etching

We synthesized Ag NPRs by the seed growth method [25]. First, Ag seeds were prepared via the reduction of Ag(I) precursor by $NaBH_4$ in the presence of citrate and PSS to control the morphology, and maintain the colloidal stability. Fig. S2 of the SI shows the optimized conditions for the preparation of Ag seeds, including the concentrations of citrate, PSS, and $NaBH_4$. Subsequently, as-prepared yellow Ag seeds were further grown by the addition of Ag(I) precusor with a mild reducing agent, AA. Figs. S3 (A), (B), and (C) of the SI show the optimized concentration of AA and volume of Ag(I) precursor—$AgNO_3$ solution—for the growth of Ag seeds to Ag NPRs. Figure S3 (B) and (C) of the SI shows that if the same volume (400 μL) of the seed solution was used for the growing, the amount and shape/size of Ag NPRs were mainly controlled by the added volume of $AgNO_3$ (0.5 mM) to the mixed solution during the growth step. The greater volume of

$AgNO_3$ that was added to the growing solution, the greater the number of and the larger the Ag NPRs that were produced. The formation of the Ag NPRs, perceived by simple visual observation of the color, was monitored by the UV-Vis spectra. As a result, Ag NPRs at the optimized conditions were grown continuously until the $LSPR_{\lambda max}$ was located at 740 nm, and the reaction was terminated. The prepared Ag NPR solution was very stable up to 14 days (Fig. S3(D) of the SI).

The Ag NPRs undergo oxidative etching due to the attack of halide ions toward the high-energy edge area (110), compared with the low-energy surface area (111) [28]. Therefore, the shape of Ag NPRs gradually changes to round Ag NPls or NDs, depending on the level of oxidative etching. Figure 1a shows that the treatment of 1 M KCl for 10 min shifted the $LSPR_{\lambda max}$ from 740 to 410 nm (black to red lines, respectively). The color of the solution changed from blue to yellow. These results prove the ability of KCl as a powerful etchant to convert triangular Ag NPRs to round shape or Ag nanoparticles (Ag NPs).

To characterize the change in triangular Ag NPRs on the paper substrate by KCl, we performed SEM measurement, Raman spectroscopy, and colorimetric analysis, respectively. Prior to the characterization of Ag NPRs on the paper, we optimized the drop volume of Ag NPRs solution on the paper. As shown in Fig. S4 of the SI, the intensity of parameter b in the L*a*b color space of Ag NPRs on the paper without any treatment did not change according to the drop volume from (3 to 8) μL. But, after 1 M KCl treatment, the parameter b intensity of Ag NPRs on the detection zone gradually increased with increasing drop volume of Ag NPRs solution. Therefore, we selected the drop volume of Ag NPRs on the detection zone in the paper substrate as 7 μL, considering the large difference in color intensity of Ag NPRs without and with 1 M KCl treatment.

First, we characterized the color change in Ag NPRs-coated paper substrates by the KCl treatment. Figure 1b shows the intensity of parameter b and color image of Ag NPRs-coated paper substrates before and after KCl treatment. The figure shows that after KCl treatment, the blue color of Ag NPRs on the paper was converted to the yellow color, demonstrating the etching of the Ag NPRs by Cl^- ion. This color change in Ag NPRs increased the parameter b intensity from -10.01 ± 0.15 to 34.79 ± 0.88. Therefore, we confirmed that

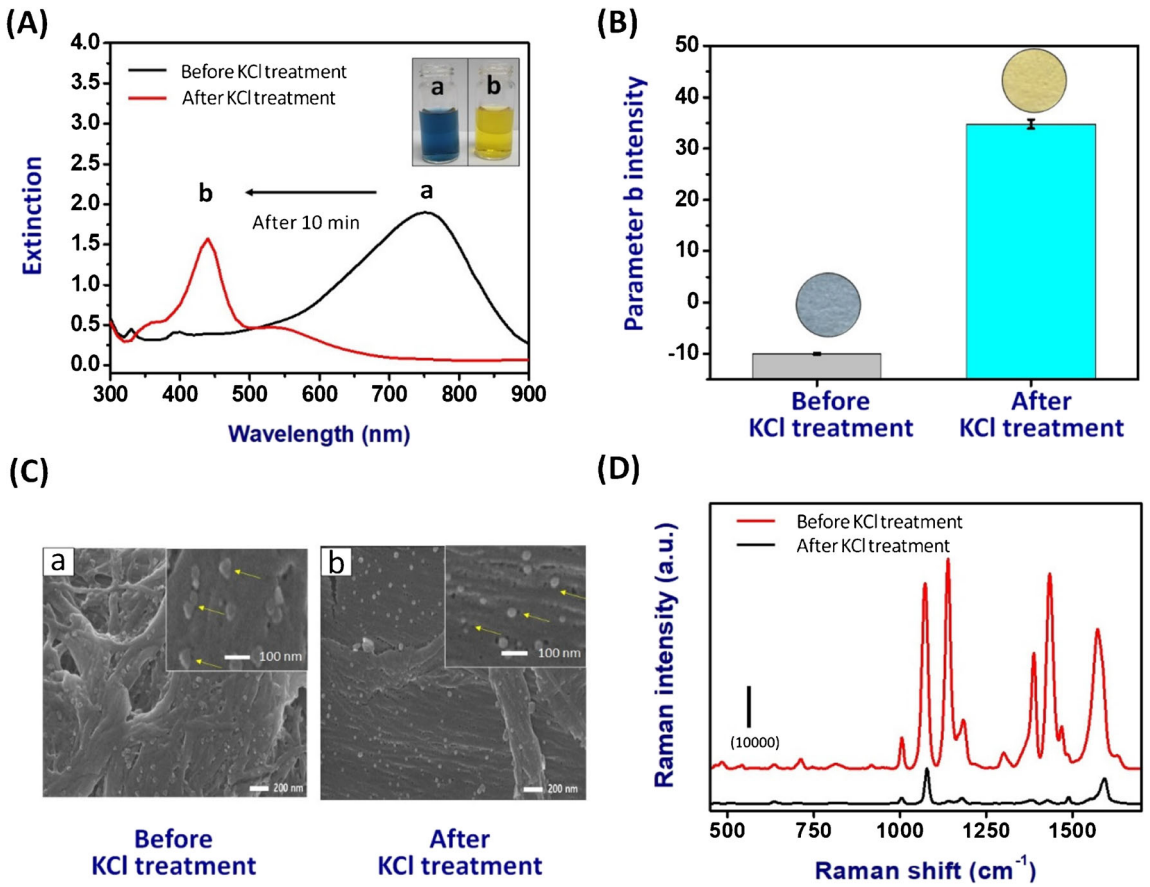

Fig. 1 Characterization of silver nanoprisms (Ag NPRs) before and after KCl treatment. (**a**) UV-Vis spectra and photographic images of the colloidal silver nanoprisms (Ag NPRs) solutions (a) before, and (b) after, 1 M KCl treatment for 10 min. (**b**) The color change in Ag NPRs-coated paper substrates before and after 1 M KCl treatment for 10 min. (**c**) SEM imagery of Ag NPRs on the paper substrate (a) before, and (b) after, 1 M KCl treatment. (**d**) Raman spectra of 1 mM 4-ATP on Ag NPR-coated paper before (red line), and after (black line), 1 M KCl treatment

KCl could change the color intensity of Ag NPR-coated paper by etching the Ag NPRs effectively. Figure 1c shows the SEM images of Ag NPRs coated on the paper substrate before and after treatment of 1 M KCl. The figure shows that without any treatment, Ag NPRs with $LSPR_{\lambda max}$ of 740 nm exhibited the triangular shape having an edge length of approximately 50 nm on the paper. But, after treatment of 1 M KCl, triangular Ag NPRs were converted into round-type Ag NDs or Ag NPs. To confirm the change in the SERS activity of Ag NPRs by the KCl treatment, Raman spectra of 1 mM 4-ATP were obtained from the Ag NPR-coated paper before and after the 1 M KCl treatment. Table 1 provides the detailed assignment of the Raman peaks for 4-ATP. Figure 1d shows that the Raman intensity of 1 mM 4-ATP in Ag NPR-coated paper before treatment (red line) was higher than that of the Ag NPRs-coated paper after the 1 M KCl treatment (black line). In particular, the most intense peaks of 4-ATP at (1140 and 1440) cm^{-1} were very obvious on the Ag NPR-coated paper. Ag NPRs exhibited remarkable activity for SERS, which was attributed to strong electromagnetic fields at the corners [29]. However, the treatment of KCl etched the corner of triangular Ag NPRs, showing the decrease of the SERS activity of Ag NPRs.

Optimization of ag NPR-coated H_2S sensing paper

It is known that sulfur can chemically bind to the surface edge of Ag NPRs in the form of Ag_2S [30], and can protect and maintain the shape of Ag NPRs from the oxidative etching of halide ions. Therefore, in this study, we prepared Ag NPR-coated colorimetric H_2S sensing paper, utilizing the etching-resistance strategy of Ag NPRs by H_2S gas against the attack of Cl^- ion. The colorimetric H_2S sensing is based on the difference of the etching of Ag NPRs by Cl^- ion after the reaction with H_2S, resulting in the color change from yellow to purplish brown, depending on the concentration of H_2S. In previous study, we had detected H_2S using the direct color change in blue Ag NPls to brown-colored Ag_2S by the reaction with H_2S [27]. But for sufficient color change, it was necessary to react Ag NPls with H_2S for 2 h. The Ag NPR-coated H_2S sensing paper used in this study can cause the color change even within a very short reaction time, because the oxidative etching of Ag NPRs by Cl^- ion is very sensitive to the Ag_2S formed by H_2S.

Table 1 Peak assignment of Raman spectra for 4-ATP molecules

Peak (cm^{-1})	Assignment
464	C-C-C vibration mode
635	C-C-C vibration mode
827	C-N+C-S+CCC vibration mode
1007	C-C vibration mode+C-C-C vibration mode
1077	**C-S vibration mode**
1140	C-H stretching mode
1185	C-H stretching mode
1390	C-N vibration mode
1443	C-C vibration mode+C-H stretching mode
1586	C-C vibration mode

To maximize the colorimetric sensing efficiency for the H_2S gas, we optimized the fabrication conditions, including the $LSPR_{\lambda max}$ and volume of Ag NPRs, the reaction time between Ag NPRs and H_2S, and the concentration of KCl, using multi-zone patterned H_2S sensing paper for passive (diffusion) mode. First, we analyzed the color intensity of Ag NPR-coated paper according to the $LSPR_{\lambda max}$. Ag NPRs with different $LSPR_{\lambda max}$ of 560, 600, 740, 820, and 960 nm were prepared by varying the amount of seed solution, as shown in Fig. 2a. When the amount of seed solution increased, the $LSPR_{\lambda max}$ of Ag NPRs was blue shifted from 930 to 480 nm. As a result, the more the seeds, the smaller the Ag NPRs. Figure 2b represents the change in parameter b intensity of H_2S sensing-coated paper that was coated with various Ag NPRs with different $LSPR_{\lambda max}$ by the treatment of 1 M KCl, after the reaction with H_2S in the concentration range (1.03 to 32.9) μM for 1 min. The figure shows that Ag NPRs with 740 nm $LSPR_{\lambda max}$ displayed the maximum color change and the best linearity in the detection zone on the paper, according to the concentration of H_2S. Therefore, for the effective detection of H_2S, we selected Ag NPRs with 740 nm $LSPR_{\lambda max}$.

Next, we optimized the concentration of KCl for the maximum color change in Ag NPR-coated detection zone on the paper after the reaction with H_2S. Figure 2c shows that the higher concentration of KCl treated on the detection zone led to an increase in the change in color intensity according to the concentration of H_2S. This data showed that the higher concentration of KCl could effectively etch the Ag NPRs, resulting in a better color change. Therefore, we selected the treated concentration of KCl as 1 M. Finally, we investigated the effect of the reaction time of 1, 2.5, 5, 7, and 10 min between the Ag NPRs and H_2S on the change in color intensity of the detection zone. Figure 2d shows that with the increase of reaction time, the change in color intensity of Ah NPR-coated paper decreased. Therefore, we selected 1 min as the reaction time for the efficient formation of Ag_2S that could protect the etching of Ag NPRs by Cl^- ion.

Analytical performance of the Ag NPR-coated and multi-zone patterned H_2S sensing paper

We evaluated the analytical performance of the Ag NPR-coated and multi-zone patterned H_2S sensing paper for the passive mode, using 96-well microplate. The color changes in the Ag NPR-coated detection zone on the paper were measured after the addition of various concentrations of Na_2S (as a

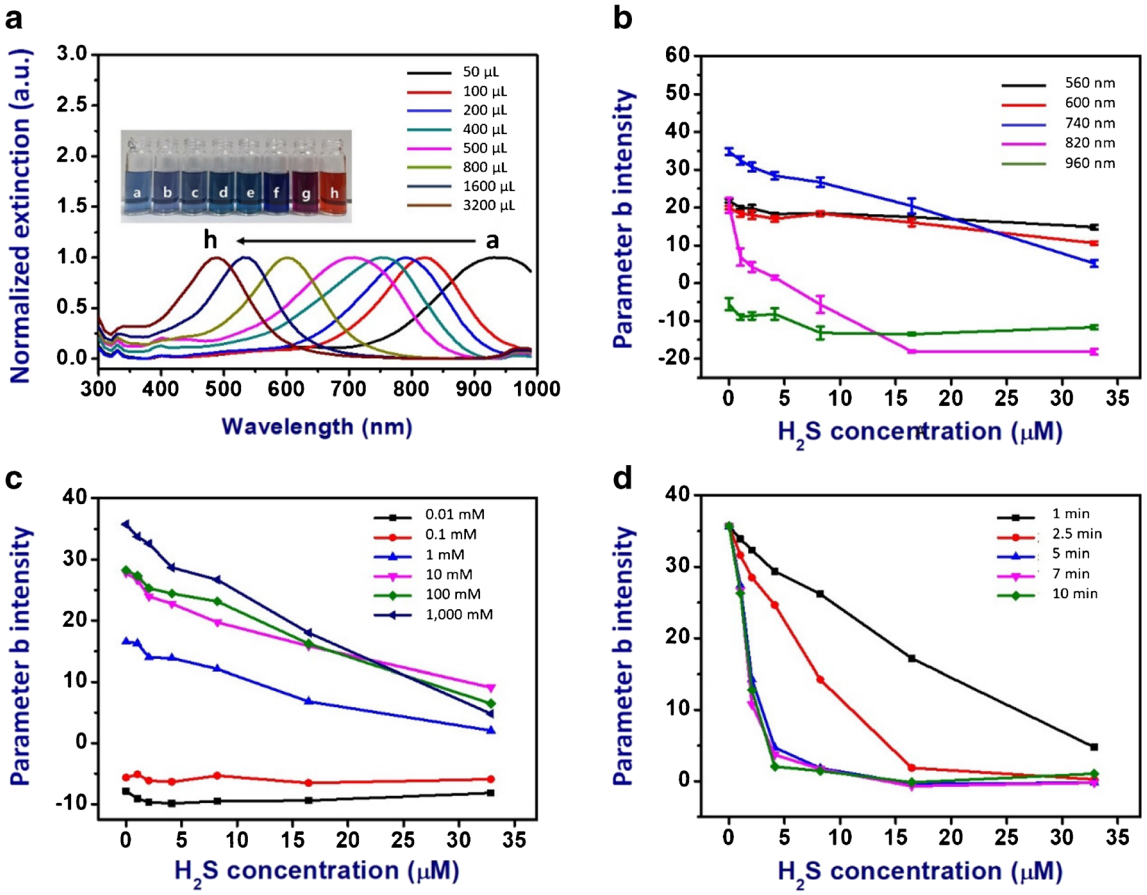

Fig. 2 (**a**) UV-Vis spectra and photographic images of the colloidal silver nanoprisms (Ag NPRs) solutions obtained from different volumes of seeds. Changes in parameter b intensity of the multi-zone patterned H_2S sensing paper depending on the concentration of H_2S in phosphate buffered saline according to (**b**) different maximum localized surface plasmon resonance wavelengths (LSPR $_{\lambda max}$) of 560, 600, 740, 820, and 960 nm, (**c**) the treatment concentration of KCl of 0.01, 0.1, 1, 10, 100, and 1000 mM, and (**d**) the reaction time of 1, 2.5, 5, 7, and 10 min between Ag NPRs and H_2S

H_2S donor) solution in PBS to each well for 1 min at RT. Figure 3a shows that the concentration of H_2S changed the color intensity of the Ag NPR-coated detection zone on the paper without any treatment very little, showing a similar blue color. But, after KCl treatment, the intensity of parameter b decreased with an increase in H_2S concentration, showing a linear relationship with H_2S concentration ranging 1.03 to 32.9 µM ($R^2 = 0.989$). With an increase in H_2S concentration, the color of Ag NPRs changed from yellow to purplish brown. The sensitivity of Ag NPl-coated H_2S sensing paper for the passive mode was 0.85 parameter b intensity per µM H_2S, which was about 28 times higher than that without the KCl treatment (0.03 parameter b intensity per µM H_2S). The limit of detection (LOD) was found to be 3.13 µM H_2S in PBS, according to the standard deviation of the blank and the slope method (3 s_{bl}/slope) [31].

To evaluate the selectivity of the prepared colorimetric H_2S sensing paper, we tested the color intensity of Ag NPR-coated detection zone after the addition of four kinds of sulfur-containing compounds (1 mM), namely DTT, GSH, H-Cys, and Cys, together with 1 mM $NaNO_2$ as a nitric oxide donor. Figure 3b shows that only H_2S caused a dramatic change in color intensity, showing the protective effect of H_2S on Ag NPRs against the etching by Cl^- ion. Other interferences showed yellow colors, similar to the change in the original Ag NPRs by Cl^- ion. This result clearly showed that the prepared H_2S sensing paper had high selectivity toward the H_2S gas. In addition, we investigated the reproducibility of Ag NPR-coated papers by measuring the changes in color intensity to H_2S (8.2 µM) in 12 sensing papers. Figure 3c shows that the relative standard deviation (RSD) was 4.8%. This result showed that the H_2S sensing papers were highly reproducible. The stability of our H_2S sensing paper was tested by evaluating the changes in color intensity of Ag NPRs to H_2S, as well as KCl treatment only, for 14 days of storage at RT without light and air. Figure 3d shows that there was no significant change in the colorimetric detection at 14 days (~99% of the initial response in Ag NPRs, ~97% of the initial response in Ag NPRs with KCl treatment, and ~ 86% of the initial response in Ag NPRs with KCl treatment after the

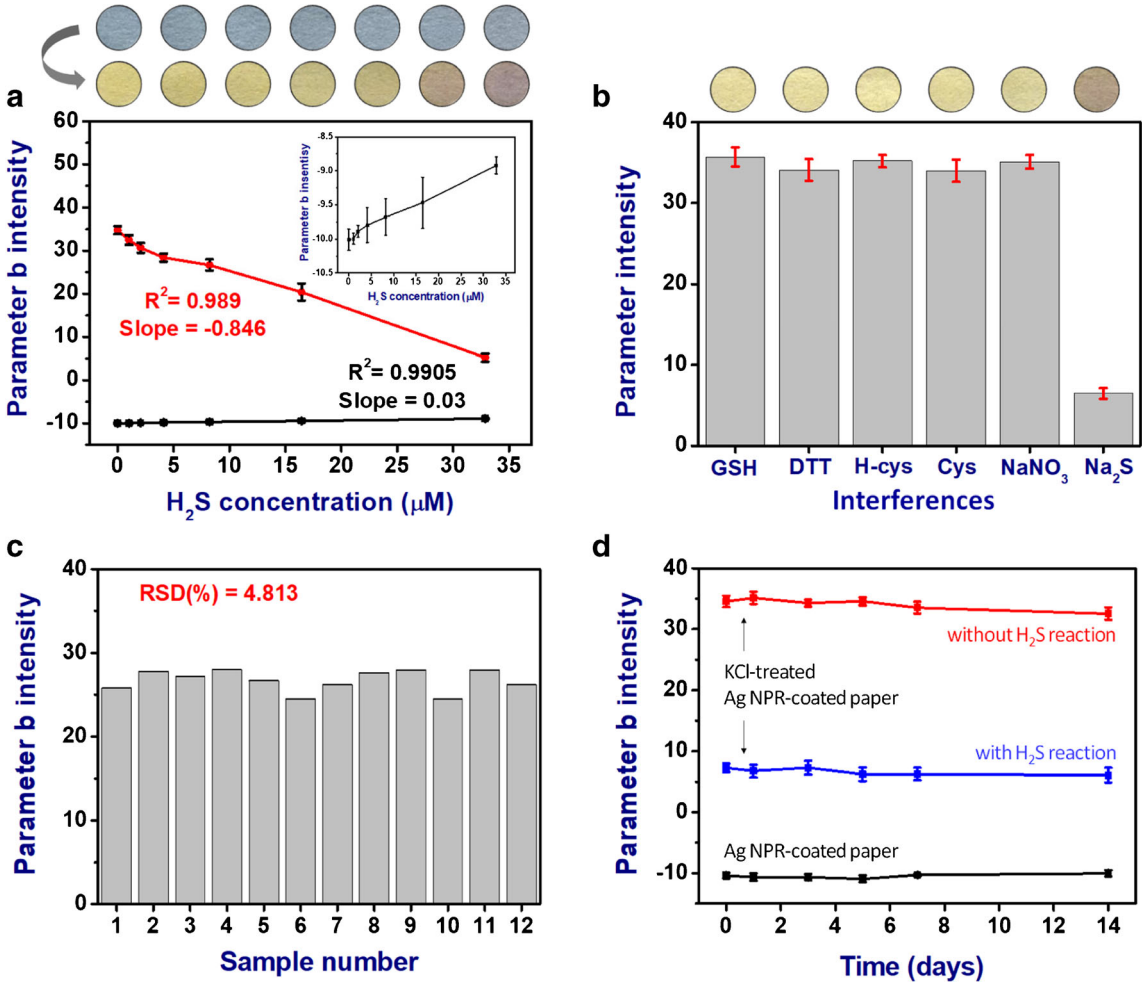

Fig. 3 The analytical performance of the silver nanoprism (Ag NPR)-coated and multi-zone patterned H_2S sensing paper. (**a**) Calibration plot of parameter b intensity versus concentration of H_2S in phosphate buffered saline for the Ag NPR-coated, multi-zone patterned paper at RT for 1 min, without (black line, inset), and with, KCl treatment (red line). The images represent the color changes in the detection zone of Ag NPR-coated paper after reaction with different concentrations of H_2S for 1 min without (upper row), and with, KCl treatment (bottom row). (**b**) Changes in parameter b intensity of the multi-zone patterned H_2S sensing paper with KCl treatment after reaction with 16.4 μM H_2S and 1 mM of other sulfur-containing compounds, including glutathione (GSH), dithiothreitol (DTT), homocysteine (H-cys), and cysteine (Cys), as well as $NaNO_2$ (nitric oxide donor). (**c**) Reproducibility of changes in parameter b intensity of 12 Ag NPR-coated papers after exposure to H_2S (8.2 μM). (**d**) Stability of Ag NPR-coated multi-zone patterned H_2S sensing paper during 14 days of storage at RT under controlled condition without light and air. Each line represents the color intensity change in Ag NPR-coated paper (black line) and KCl-treated Ag NPR-coated paper without (red line), and with (blue line), the reaction of H_2S, respectively

reaction with H_2S, respectively). Therefore, the proposed H_2S sensing paper has good stability under controlled storage conditions.

The sample collection for Ag NPR-coated and a single-zone patterned H_2S sensing paper

To detect the H_2S gas for pumped mode, we prepared a single-zone patterned H_2S sensing paper, which was inserted within a holder, and connected to a syringe and pump. Because the H_2S gas within the beaker was collected by syringe, we optimized the sample collection conditions, including the accumulation time for H_2S gas released from the H_2S donor solution, and the reaction volume of H_2S gas. To determine the optimal accumulation time for H_2S gas, we measured the change in color intensity of Ag NPR-coated and single-zone patterned H_2S sensing paper according to the concentration range from 1.03 to 32.9 μM H_2S at each accumulation time of 5, 10, 20, and 40 min. Figure 4a shows that the calibration curve revealed good linearity to H_2S, which was collected after the accumulation for 20 min, compared with those of other accumulation times. Therefore, we selected the accumulation time for H_2S as 20 min.

Next, we optimized the reaction volume of H_2S gas with the prepared H_2S sensing paper by varying the volume from 5.5 to 10 mL. Figure 4b shows that the change in the color intensity of Ag NPR-coated H_2S sensing paper showed the best linearity in the concentration range from 1.03 to 32.9 μM

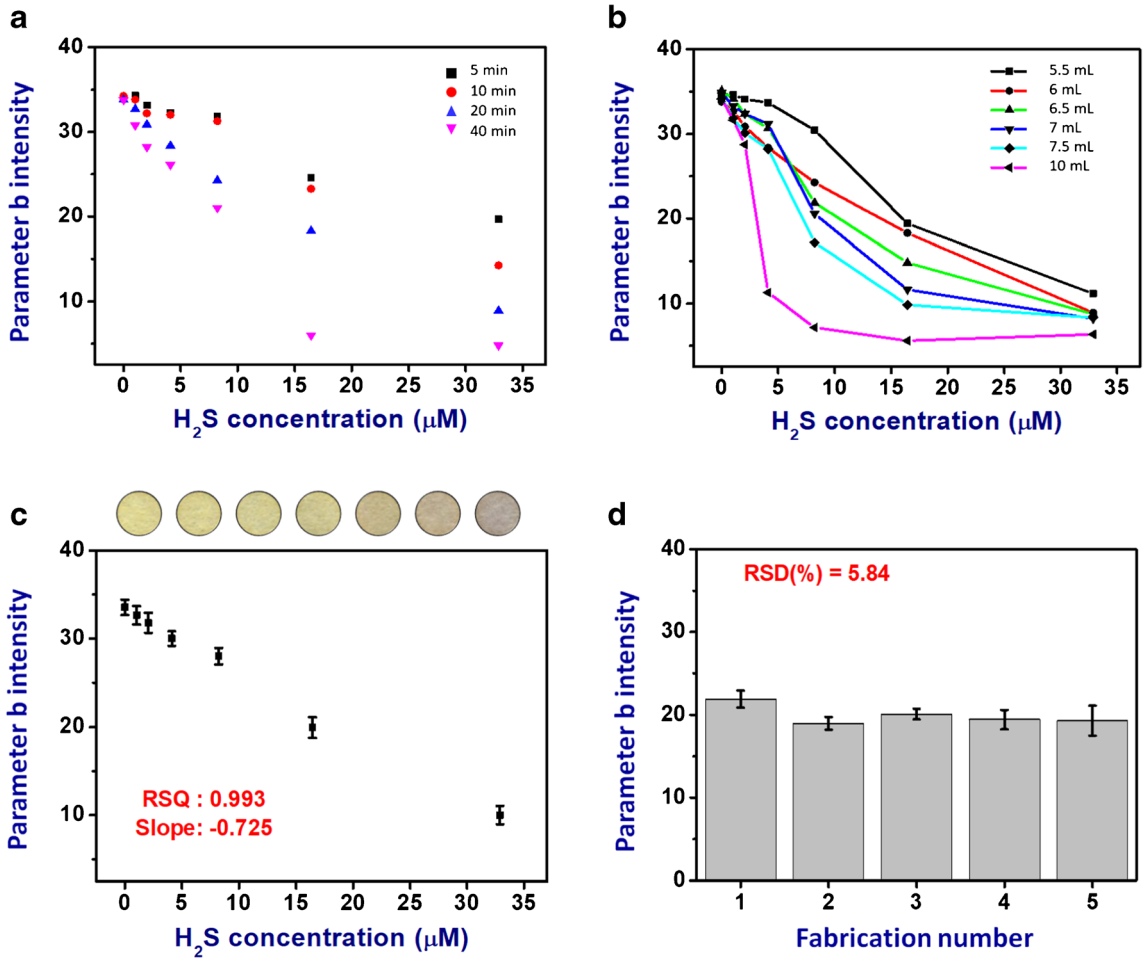

Fig. 4 Optimization and analytical performance of silver nanoprism (Ag NPR)-coated and single-zone patterned H_2S sensing paper. The changes in parameter B intensity of Ag NPR-coated, single-zone patterned paper depending on the H_2S concentration at (**a**) different accumulation time of 5, 10, 20, and 40 min for H_2S gas in 500 mL beaker, and (**b**) different reaction volume of 5.5, 6, 6.5, 7, 7.5, and 10 mL of H_2S gas within the holder. (**c**) Calibration plot of parameter b intensity versus concentration of H_2S in phosphate buffered saline for the Ag NPR-coated, single-zone patterned paper at RT for 1 min with KCl treatment. (**d**) Reproducibility of changes in parameter b intensity of a total of 20 Ag NPR-coated papers performed on 5 different fabrication dates after exposure to 16.4 μM H_2S

H_2S at 6 mL of H_2S gas. Therefore, we selected the reaction volume of H_2S gas for the single-zone patterned H_2S sensing paper as 6 mL.

Analytical performance of the Ag NPR-coated and a single-zone patterned H_2S sensing paper

To evaluate the analytical performance of Ag NPR-coated H_2S sensing paper, the color change in a single detection zone on the paper was measured after the injection of H_2S gas at the concentration range from 1.03 to 32.9 μM for 1 min. Similar to the multi-zone patterned paper for the passive mode, 1 M KCl treatment turned the blue-colored Ag NPRs without H_2S exposure yellow. But, after the reaction with H_2S, with an increase in H_2S concentration, they turned from yellow to brown/purple (Fig. 4c). The prepared H_2S sensing paper showed good linearity in the H_2S concentration range from 1.03 to 32.9 μM ($R^2 = 0.993$). The sensitivity was 0.73 parameter b intensity per μM H_2S, and the LOD was 3.6 μM H_2S based on 3 s_{bl}/slope.

The response of the single-zone patterned H_2S sensing paper was slightly lower than that of the multi-zone patterned paper (slope: 0.85 parameter b intensity per μM H_2S) in the concentration range from 1.03 to 32.9 μM H_2S (Fig. S5 of the SI). However, the sensitivity values of the two types of H_2S sensing paper were the same (1.2 parameter b intensity per μM H_2S) in the H_2S concentration range from 1.03 to 16.4 μM. Furthermore, the RSD of the prepared H_2S sensing paper was 5.84% (Fig. 4d). This result indicates that the Ag NPR-coated and single-patterned paper both showed good reproducibility.

Comparison with a commercially available lead acetate paper for the detection of H_2S

Lead acetate test paper is used to detect H_2S produced by microorganisms, and to evaluate the quality of water and food

[32]. The H_2S sensing is based on the specific reactivity of lead acetate with H_2S, resulting in a brown lead sulfide stain. To compare the sensitivity of our Ag-NPR-coated paper with the lead acetate paper, the changes in the color intensity of two sensing papers were measured after the exposure to H_2S for 1 min, using a 96-well microplate. Figure 5a shows that with an increase in H_2S concentration, the color of the lead acetate paper changed slightly from white to pale yellow. However, it was difficult to easily identify with the naked eye the color change of the paper. Therefore, we analyzed the image using the blue channel of the RGB (red, green, blue) model. Figure 5 shows that the change in the blue channel intensity of lead acetate paper revealed a linear relationship with H_2S concentration ranging from 1.03 to 32.9 μM ($R^2 = 0.99$). But the standard deviation of each value was very high, showing low reproducibility. The LOD was 11.3 μM H_2S (based on 3 s_{bl}/slope), which was 3.6 times higher than that of our Ag NPR-coated paper (3.1 μM H_2S). As a result, Ag NPR-coated H_2S sensing paper showed higher sensitivity and reproducibility, compared to lead acetate test paper.

Feasibility test

Garlic is rich in organosulfur compounds, which are known to be responsible for most of its pharmacological activities. In particular, garlic consumption has been related to the reduction in multiple risk factors associated with cardiovascular diseases, such as increased reactive oxygen species, high blood pressure, high cholesterol, platelet aggregation, and blood coagulation [33, 34]. The vasoactivity of garlic compounds is synchronous with H_2S production, and their potency to mediate relaxation increases with H_2S yield [33]. Therefore, the capacity to produce H_2S can be used to standardize garlic dietary supplements.

To evaluate the feasibility of the Ag NPR-coated H_2S sensing paper, it was applied to monitor H_2S gas produced from three kinds of garlic including crushed, peeled, and fresh

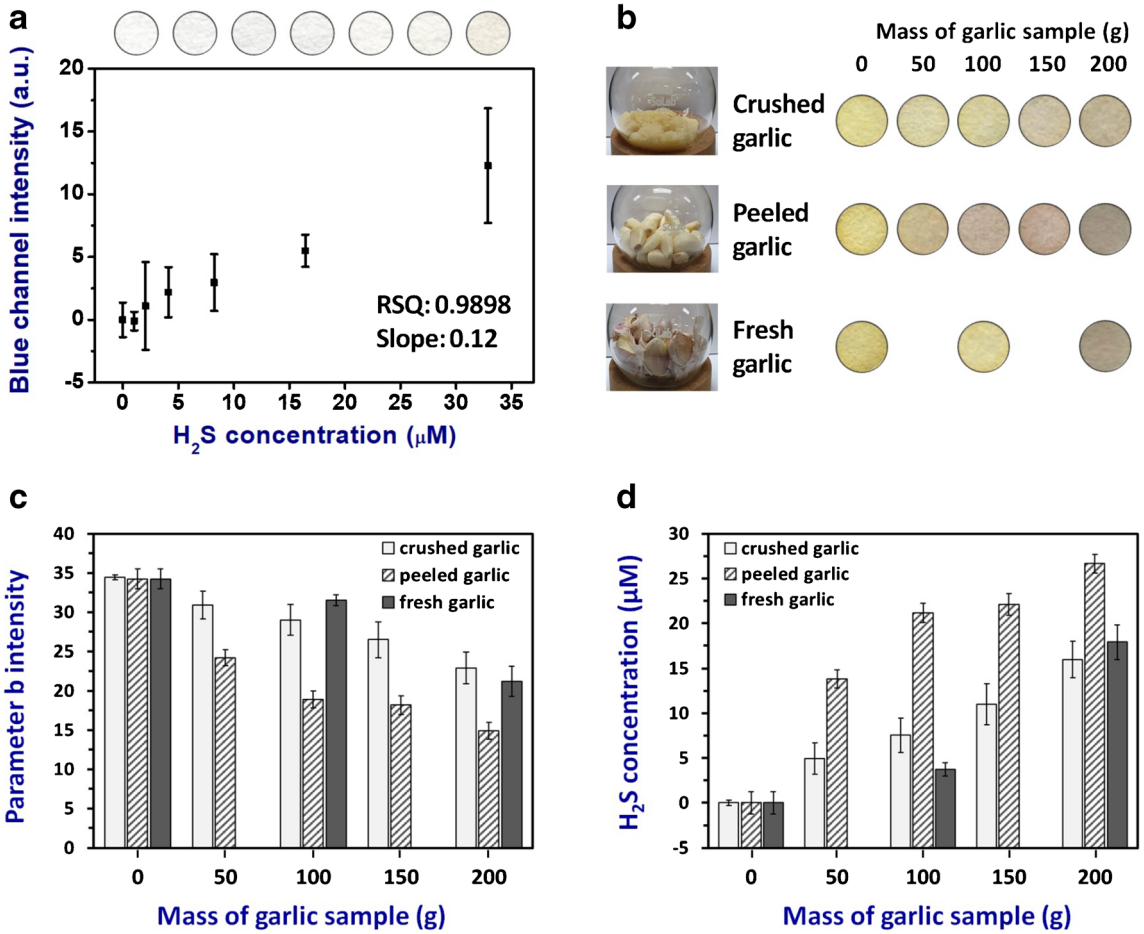

Fig. 5 (**a**) Changes in blue channel intensity of a commercially available lead acetate paper after the exposure to H_2S for 1 min, using a 96-well microplate. (**b**) Color changes in the detection zone of silver nanoprism (Ag NPR)-coated, single-zone patterned H_2S sensing paper after exposure to each H_2S gas for 1 min, collected from the various mass of three kinds of garlic including crushed, peeled, and fresh garlic, using a syringe. (**c**) Changes in parameter b intensity and (**d**) quantitative analysis of H_2S production released from the various mass of crushed, peeled, and fresh garlic, respectively

garlic. The change in color intensity of our H_2S sensing paper was measured from gas samples that were collected from the various mass of 50, 100, 150, and 200 g of crushed and peeled garlic, and 100 and 200 g of fresh garlic, respectively, using a syringe. The reaction time between Ag NPRs and H_2S gas was 1 min. Figures 5b-d show that higher amounts of crushed and peeled garlic could release more H_2S gas (4.9 ± 2.4, 7.5 ± 2.7, 11.0 ± 3.1, and 16.0 ± 2.8 μM from 50, 100, 150, and 200 g crushed garlic, respectively; 13.8 ± 1.4, 21.2 ± 1.5, 22.1 ± 1.7, and 26.6 ± 1.4 μM from 50, 100, 150, and 200 g peeled garlic, respectively), showing color changes in the detection zone from yellow to purplish brown. Besides, the H_2S concentration released from 100 and 200 g fresh garlic was 3.7 ± 1.0 and 17.9 ± 2.7 μM, respectively. These results showed that Ag NPR-coated H_2S sensing paper could successfully detect H_2S gas produced from the different mass of various garlic samples.

Conclusion

In this paper, we developed a fast, simple, and sensitive H_2S sensing paper using Ag NPRs, which possess a specific optical property due to their extreme geometric anisotropy. As the formation of Ag_2S after the reaction with H_2S gas on Ag NPRs showed the effective etching-resistant effect on Ag NPRs against Cl^- ion, the color of Ag NPR-coated paper changed after KCl treatment from blue to purplish brown. We prepared two types of Ag NPRs-coated paper sensor for H_2S sensing, such as the multi-zone patterned H_2S sensing paper for passive (diffusion) mode, and the single-zone patterned H_2S sensing paper for pumped mode, depending on the reaction mode between Ag NPRs and H_2S gas. These Ag NPR-coated papers can simply detect H_2S after the sequential reaction with H_2S gas and KCl. Both Ag NPR-coated H_2S sensing papers showed high sensitivity, good selectivity, high reproducibility, and good stability, as well as fast reaction time (1 min) between Ag NPRs and free H_2S gas. We successfully measured the H_2S level released from the different amounts of crushed, peeled, and fresh garlic. Therefore, we suggest that these H_2S sensing papers demonstrate great potential for providing quality control of dietary supplements, and application to exhaled breath analysis for the noninvasive diagnosis of halitosis.

Supplementary Information The online version contains supplementary material available at https://doi.org/10.1007/s00604-021-04783-4.

Acknowledgements This research was supported by National Research Foundation grant funded by the Korean government (No. NRF-2018R1A2B6007635) and the Korea Medical Device Development Fund grant funded by the Korea government (the Ministry of Science and ICT, the Ministry of Trade, Industry and Energy, the Ministry of Health & Welfare, Republic of Korea, the Ministry of Food and Drug Safety) (Project Number: KMDF_PR_20200901_0023, 9991006696).

Declaration

Conflict of interest The authors declare no conflict of interest.

References

1. Powell CR, Dillon KM, Matson JB (2018) A review of hydrogen sulfide (H_2S) donors: chemistry and potential therapeutic applications. Biochem Pharmacol 149:110–123. https://doi.org/10.1016/j.bcp.2017.11.014
2. Policastro MA, Otten EJ (2007) Case files of the University of Cincinnati fellowship in medical toxicology: two patients with acute lethal occupational exposure to hydrogen sulfide. J Med Toxicol 3:73–81. https://doi.org/10.1007/BF03160912
3. Doujaiji B, Al-Tawfiq JA (2010) Hydrogen sulfide exposure in an adult male. Ann Saudi Med 30:76–80. https://doi.org/10.4103/0256-4947.59379
4. Yang G, Wu L, Jiang B, Yang W, Qi J, Cao K, Meng Q, Mustafa AK, Mu W, Zhang S, Snyder SH, Wang R (2008) H_2S as a physiologic vasorelaxant: hypertension in mice with deletion of cystathionine γ-lyase. Science 322:587–590. https://doi.org/10.1126/science.1162667
5. Abe K, Kimura H (1996) The possible role of hydrogen sulfide as an endogenous neuromodulator. J Neurosci 16:1066–1071. https://doi.org/10.1523/JNEUROSCI.16-03-01066.1996
6. Jin S, Pu SX, Hou CL, Ma FF, Li N, Li XH, Tan B, Tao BB, Wang MJ, Zhu YC (2015) Cardiac H_2S generation is reduced in ageing diabetic mice. Oxidative Med Cell Longev 2015:758358–758314. https://doi.org/10.1155/2015/758358
7. Eto K, Asada T, Arima K, Makifuchi T, Kimura H (2002) Brain hydrogen sulfide is severely decreased in Alzheimer's disease. Biochem Biophys Res Commun 293:1485–1488. https://doi.org/10.1016/S0006-291X(02)00422-9
8. Florin THJ, Neale G, Goretski S, Cummings JH (1993) The sulfate content of foods and beverages. J Food Compos Anal 6:140–151. https://doi.org/10.1006/jfca.1993.1016
9. Banik GD, De A, Som S, Jana S, Daschakraborty SB, Chaudhuri S et al (2016) Hydrogen sulphide in exhaled breath: a potential biomarker for small intestinal bacterial overgrowth in IBS. J Breath Res 10:026010. https://doi.org/10.1088/1752-7155/10/2/026010
10. Aylikci BU, Çolak H (2013) Halitosis: from diagnosis to management. J Nat Sci Biol Med 4:14–23. https://doi.org/10.4103/0976-9668.107255
11. Xu T, Scafa N, Xu LP, Zhou S, Abdullah Al-Ghanem K, Mahboob S et al (2016) Electrochemical hydrogen sulfide biosensors. Analyst 141:1185–1195. https://doi.org/10.1039/c5an02208h
12. Ding Y, Li X, Chen C, Ling J, Li W, Guo Y, Yan J, Zha L, Cai J (2017) A rapid evaluation of acute hydrogen sulfide poisoning in blood based on DNA-cu/ag nanocluster fluorescence probe. Sci Rep 7:1–9. https://doi.org/10.1038/s41598-017-09960-1
13. Lewis A (2010) Review of metal sulfide precipitation. Hydrometallurgy 104:222–234. https://doi.org/10.1016/j.hydromet.2010.06.010
14. Olson KR (2012) A practical look at the chemistry and biology of hydrogen sulfide. Antioxid Redox Signal 17:32–44. https://doi.org/10.1089/ars.2011.4401
15. Shen X, Pattillo CB, Pardue S, Bir SC, Wang R, Kevil CG (2011) Measurement of plasma hydrogen sulfide in vivo and in vitro. Free Radic Biol Med 50:1021–1031. https://doi.org/10.1016/j.freeradbiomed.2011.01.025

16. Kaushik R, Ghosh A, Singh A, Jose DA (2018) Colorimetric sensor for the detection of H_2S and its application in molecular half-subtractor. Anal Chim Acta 1040:177–186. https://doi.org/10.1016/j.aca.2018.08.028
17. Wang H, Wu X, Yang S, Tian H, Liu Y, Sun B (2019) A visible colorimetric fluorescent probe for hydrogen sulfide detection in wine. Food Chem 286:322–328. https://doi.org/10.1016/j.foodchem.2019.02.033
18. Lee BH, Hsu MS, Hsu YC, Lo CW, Huang CL (2010) A facile method to obtain highly stable silver nanoplate colloids with desired surface plasmon resonance wavelengths. J Phys Chem 114:6222–6227. https://doi.org/10.1021/jp910100k
19. Zhang Q, Li N, Goebl J, Lu Z, Yin Y (2011) A systematic study of the synthesis of silver manoplates: is citrate a "magic" reagent? J Am Chem Soc 133:18931–18939. https://doi.org/10.1021/ja2080345
20. Chen Z, Zhang C, Wu Q, Li K, Tan L (2015) Application of triangular silver nanoplates for colorimetric detection of H_2O_2. Sens Actuator B-Chem 220:314–317. https://doi.org/10.1016/j.snb.2015.05.085
21. Tang B, An J, Zheng X, Xu S, Li D, Zhou J, Zhao B, Xu W (2008) Silver nanodisks with tunable size by heat aging. J Phys Chem C 112:18361–18367. https://doi.org/10.1021/jp806486f
22. Zhang Q, Ge J, Pham T, Goebl J, Hu Y, Lu Z, Yin Y (2009) Reconstruction of silver nanoplates by UV irradiation: tailored optical properties and enhanced stability. Angew Chem Int Ed Engl 48:3516–3519. https://doi.org/10.1002/anie.200900545
23. Zhang P, Wang L, Zeng J, Tan J, Long Y, Wang Y (2020) Colorimetric captopril assay based on oxidative etching-directed morphology control of silver nanoprisms. Microchim Acta 187:107. https://doi.org/10.1007/s00604-019-4071-8
24. Li Y, Li Z, Gao Y, Gong A, Zhang Y, Hosmane NS et al (2014) "Red-to-blue" colorimetric detection of cysteine via anti-etching of silver nanoprisms. Nanoscale 21:10631–10637. https://doi.org/10.1039/c4nr0..09d
25. Aherne D, Deirdre DM, Gara M, Kelly JM (2008) Optical properties and growth aspects of silver naniprisms produced by a highly reproducible and rapid synthesis at room temperature. Adv Funct Mater 18:2005–2016. https://doi.org/10.1002/adfm.200800233
26. Lee J, Lee YJ, Ahn YJ, Choi S, Lee GJ (2018) A simple and facile paper-based colorimetric assay for detection of free hydrogen sulfide in prostate cancer cells. Sens Actuator B-Chem 256:828–834. https://doi.org/10.1016/j.snb.2017.10.019
27. Ahn YJ, Gil YG, Lee YJ, Jang H, Lee GJ (2020) A dual-mode colorimetric and SERS detection of hydrogen sulfide in live prostate cancer cells using a silver nanoplate-coated paper assay. Microchem J 155:104724. https://doi.org/10.1016/j.microc.2020.104724
28. Gu Y, Kong S, Diao X, Guo Y, Zhang K, He H (2016) Mechanistic study on the facet etching effect of silver nanoprisms in the presence of halide ions and their application in the colorimetric sensing of metformin hydrochloride. New J Chem 40:7557–7563. https://doi.org/10.1039/c6nj00361c
29. Yang Y, Zhong XL, Zhang Q, Blackstad LG, Fu ZW, Li ZY, Qin D (2014) The role of etching in the formation of ag nanoplates with straight, curved and wavy edges and comparison of their SERS properties. Small 10:1430–1437. https://doi.org/10.1002/smll.201302877
30. Zeng J, Tao J, Su D, Zhu Y, Qin D, Xia Y (2011) Selective sulfuration at the corner sites of a silver nanocrystal and its use in stabilization of the shape. Nano Lett 11:3010–3015. https://doi.org/10.1021/nl2016448
31. Taverniers I, De Loose M, Van Bockstaele E (2004) Trends in quality in the analytical laboratory. II. Analytical method validation and quality assurance. Trac-Trends Anal Chem 23:535–552. https://doi.org/10.1016/j.trac.2004.04.001
32. Mironov A, Seregina T, Nagornykh M, Luhachack LG, Korolkova N, Lopes LE, Kotova V, Zavilgelsky G, Shakulov R, Shatalin K, Nudler E (2017) Mechanism of H_2S-mediated protection against oxidative stress in *Escherichia coli*. Proc Natl Acad Sci U S A 114:6022–6027. https://doi.org/10.1073/pnas.1703576114
33. Benavides GA, Squadrito GL, Mills RW, Patel HD, Scott Isbell T, Patel RP et al (2007) Hydrogen sulfide mediates the vasoactivity of garlic. Proc Natl Acad Sci U S A 104:17977–17982. https://doi.org/10.1073/pnas.0705710104
34. Banerjee SK, Maulik SK (2002) Effect of garlic on cardiovascular disorders: a review. Nutr J 1:4. https://doi.org/10.1186/1475-2891-1-4